Developmental Biology 341 (2010) 256–266

Contents lists available at ScienceDirect

Developmental Biology

journal homepage: www.elsevier.com/developmentalbiology

Evolution of Developmental Control Mechanisms

Mesoderm and ectoderm lineages in the crustacean *Parhyale hawaiensis* display intra-germ layer compensation

Alivia L. Price [a,b,1,2], Melinda S. Modrell [a,2,3], Roberta L. Hannibal [a], Nipam H. Patel [a,*]

[a] University of California-Berkeley, Departments of Molecular and Cell Biology, Integrative Biology, Center for Integrative Genomics, and HHMI, 3060 VLSB # 3140, Berkeley, CA 94720-3140, USA
[b] University of Chicago, Department of Molecular Genetics and Cell Biology, Committee on Developmental Biology, Chicago, IL 60637, USA

ARTICLE INFO

Article history:
Received for publication 14 September 2009
Revised 4 December 2009
Accepted 4 December 2009
Available online 21 December 2009

Keywords:
Parhyale
Cell lineage
Germ layer specification
Intra-germ layer compensation
Cell ablations

ABSTRACT

In *Parhyale hawaiensis*, the first three divisions are holoblastic and asymmetric, resulting in an embryo comprised of eight cells—four macromeres and four micromeres. Lineage studies performed at this stage demonstrate that the progeny of each cell contribute to specific portions of different germ layers. However, it is not known if this lineage pattern means a given blastomere is committed to its specific fate, indicative of mosaic development, or if regulation can occur between blastomere progeny so that the loss of a blastomere could be compensated for during development. Furthermore, if compensation occurs, what would be the source of such replacement? To investigate these possibilities, we performed ablation experiments at the eight-cell stage. We find that loss of blastomeres results in compensation. To determine the compensation pattern, we combined ablation and cell lineage tracing to reveal that progeny of mesoderm and ectoderm producing blastomeres display intra-germ layer compensation. Furthermore, by ablating lineages later in development, we identify a key interval between gastrulation and germband elongation after which compensation no longer occurs. Our results suggest that *Parhyale* possesses a mechanism to assess the status of mesoderm and ectoderm formation and alter development to replace the missing portions of these lineages.

Introduction

The three germ layers – ectoderm, mesoderm and endoderm – are traditionally defined during gastrulation when embryonic cells are committed to a single germ layer. In some animals, germ layer commitment can be traced through cell lineages well before gastrulation and stereotypical cleavage patterns are tightly linked to cell fate. In these animals, gastrulation acts on a prefigured canvas where germ layers have already been established by early cleavage events. This type of development is historically known as “mosaic” development whereby a cell only develops according to its lineage and an ablated cell's lineage cannot be replaced within the developing embryo. Mosaic development is typically observed in invertebrates with holoblastic or complete cleavage, such as ascidians or nematodes, where single cell lineages can be followed from early stages (Bates and Jeffery, 1988; Speksnijder et al., 1989; Sulston et al., 1983).

In other cases, germ layer formation occurs by inductive events acting upon cells in the blastula, and it is cell–cell signaling rather than ancestry that decides their ultimate fate. Thus, cell fate is a consequence of cell interactions and morphogen gradients that pattern the early embryo, as is seen from classic examples of development in the frog *Xenopus laevis* and the fruit fly *Drosophila melanogaster* (Anderson et al., 1985; Rushlow et al., 1989; Spemann and Mangold, 1924). This type of development is historically termed “regulative” development whereby the loss of an early cell can be compensated for by the embryo and normal development observed. However, no embryo can truly be classified as completely “mosaic” or “regulative” (Lawrence and Levine, 2006). In reality, most embryos studied to date employ both strategies. For instance, *Xenopus* embryos do have early segregation of cytoplasmic determinants and *C. elegans* also uses cell–cell interactions to induce early cell fates (Levin et al., 2002; Schnabel, 1997; Zhang et al., 1998).

Recently, in-depth cell lineage data have been obtained for several malacostracan crustaceans that display holoblastic cleavage: the ridgeback prawn *Sicyonia ingentis* and two amphipods *Parhyale hawaiensis* and *Orchestia cavimana* (Gerberding et al., 2002; Hertzler and Clark, 1992; Wolff and Scholtz, 2002). These studies show that, from early cleavage stages, cell lineages within these crustaceans are restricted with regard to germ layer fates. Blastomere separation analyses in *Parhyale* and *Sicyonia* further suggest that cell lineage plays a major role in determining cell fate in these crustaceans (Extavour, 2005; Hertzler et al., 1994). However, occasional mixing among cell lineages as well as the rare deviation from an otherwise

* Corresponding author. Fax: +1 510 643 5022.
E-mail address: nipam@berkeley.edu (N.H. Patel).
[1] Present address: The Salk Institute for Biological Studies, La Jolla, CA 92186.
[2] These authors contributed equally to this work.
[3] Present address: University of Cambridge, UK, Cambridge CB2 3DY.

0012-1606/$ – see front matter © 2009 Elsevier Inc. All rights reserved.
doi:10.1016/j.ydbio.2009.12.006

invariant cell lineage pattern shows that there is some capacity for regulation among the cell lineages (Gerberding et al., 2002; Hertzler et al., 1994). Thus, among crustaceans it is unclear whether early lineage restriction to germ layers is indicative of mosaic development or if regulation may play a role.

The first three cleavages in *Parhyale* occur in a very regular manner and result in the formation of an eight-cell embryo with four macromeres and four micromeres that give rise to highly stereotyped lineages (Gerberding et al., 2002). As summarized in Fig. 1, in *Parhyale*, the four macromere lineages will give rise to somatic mesoderm of the head anterior to maxilla 2 (mx2) plus the visceral mesoderm (Mav), right anterior ectoderm (Er), left anterior ectoderm (El) and posterior ectoderm (Ep). The four micromeres lineages will give rise to germline (g), right somatic trunk mesoderm posterior to and including mx2 (mr), endoderm (en) and left somatic trunk mesoderm posterior to and including mx2 (ml). These cell lineage studies raise the question of how early during development these cells are committed, if at all, to their subsequent germ layer fates and whether cell–cell interactions play a role in determining these fates. It is currently unknown to what extent maternal factors are unequally distributed within the *Parhyale* egg and early embryo, but experiments in which blastomeres from the two-, four- and eight-cell stages were separated suggest that there is a cytoplasmic determinant of the germline that is differentially localized during early cleavages (Extavour, 2005). Given the apparent restriction of cell fate and the potential localization of determinants during early cleavages, we set out to explore how mosaic the *Parhyale* embryo is and to what extent regulation is occurring during embryogenesis.

A classic approach to determining if development is mosaic from early stages is to ablate blastomeres and determine if the resulting embryo is deficient for structures that would have arisen from the ablated cells. *Parhyale* is a perfect candidate for such an approach because the early embryo displays a stereotypical cleavage pattern and cells can be easily identified at the eight-cell stage based on size and orientation (Gerberding et al., 2002). In this study, we focus on six of the eight blastomeres, ml, mr, Mav, El, Er and Ep, as these give rise to the readily distinguishable mesoderm and ectoderm derivatives of the embryo. The ablation of the remaining blastomeres, g and en, will be discussed elsewhere. We first ablate individual blastomeres to show that regulation does occur in *Parhyale* when progenitor cells are eliminated. We go on to show that, while regulation does occur, the embryo is mosaic in so far as blastomere progeny are only able to participate in intra-germ layer compensation such that mesoderm lineages will compensate for loss of mesoderm and ectoderm lineages will compensate for loss of ectoderm. Then, using a combination of later stage ablations and cell labeling experiments, we demonstrate how and when regulation occurs among the mesoderm and ectoderm lineages.

Materials and methods

Injection and photoablation

P. hawaiensis rearing and staging followed previously published procedures (Browne et al., 2005). To follow lineages, specific blastomeres were injected (Gerberding et al., 2002) with capped mRNA (SP6 Ambion mMessageMachine kit) encoding a nuclear localized version of DsRed (called DsRed-NLS; Price and Patel, 2008).

Photoablation of targeted cells was achieved by injection of approximately 100 pl of 25 to 50 mg/ml fluorescein isothiocyanate (FITC) covalently linked to dextran (250,000MW) (Sigma) into individual blastomeres followed by exposure of the entire embryo to the fluorescein excitation wavelength ($\lambda = 488$ nm) for 20 min (Shankland, 1984). For ablations at the eight-cell stage, cells were ablated using a Zeiss StemiSV11 Apo fluorescent dissecting scope. For ablations at gastrulation or germband elongation, cells were ablated on a Zeiss Axiophot under a Zeiss Plan-NeoFLUAR 10×/0.3 objective set to the fluorescein filter. Cells that did not contain FITC were unaffected by irradiation and cell death occurred only in cells containing high levels of FITC. Cell death following irradiation was confirmed by the cessation of cell division, which would have normally occurred approximately 90 min after the division to the eight-cell stage, and the later presence of cellular debris. This cellular debris was either absorbed into the developing gut or was shunted to the outside of the embryo where it remained as granular debris between the eggshell and embryo. Embryos exhibiting injection trauma were discarded. For the $n = x/y$ values shown throughout the results, y represent the number of embryos in which lineage injection and ablation were successful and the embryos survived to the stage required, and x represents the number of embryos that showed the indicated pattern of compensation (or in some cases, lack of compensation). For all our results, $x = y$ reflecting that *Parhyale*

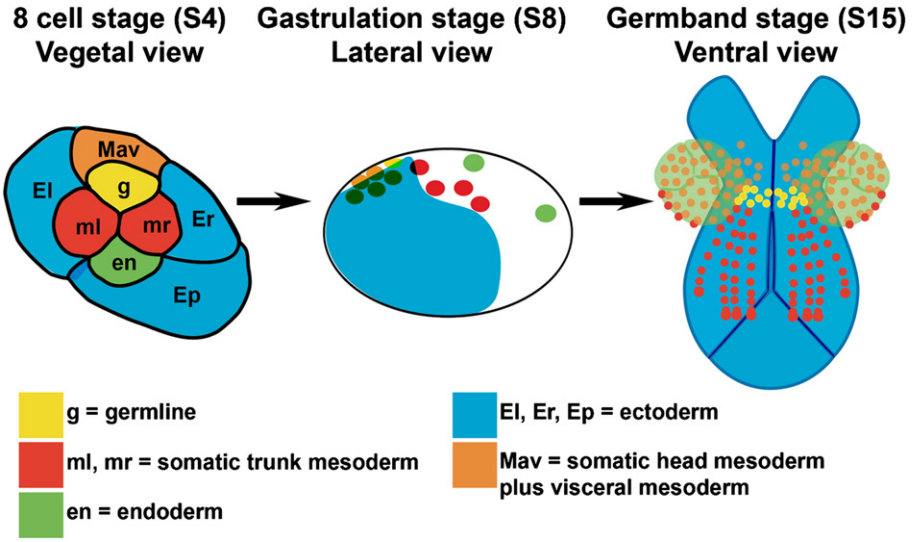

Fig. 1. Fate map of the eight-cell stage in *Parhyale*. Representation of early *Parhyale* development with blastomeres colored to indicate their lineage and eventual germ layer fate; diagram shows orientation of the blastomeres and their progeny at the eight-cell stage (S4; 7.5 hpf), gastrulation (S8; 25 hpf) and germband elongation (S15; 80 hpf). The blastomeres of the eight-cell stage are germ layer restricted and their progeny can be followed through development (Gerberding et al., 2002). View at S4 is dorsal with anterior up and posterior down. View at S8 is lateral with anterior to the left, dorsal up. View at S15 is ventral with anterior up.

embryos have a remarkably robust and precise pattern for compensation. Embryos that did not make it to the appropriate stage to be assayed generally died relatively soon after injection due to either immediate injection trauma or severe morphological damage. Embryos were prepared for microscopy as previously described (Price and Patel, 2008).

Antibody staining and in situ hybridization

Embryo fixation and *in situ* procedures were performed as described in Rehm et al. (2009). Antibody staining was performed according to Patel (1994). Primary antibody incubations were overnight at 4 °C with rabbit anti-DsRed (Clontech) at 1:1000 dilution. Secondary antibody incubations were either at 2 h at room temperature or overnight at 4 °C with HRP-conjugated goat anti-rabbit (Jackson ImmunoResearch) at 1:300–1:800 dilution. Following histochemical reaction in DAB with nickel chloride, embryos were counterstained with 1 μg/ml DAPI in 50% glycerol and transferred to 70% glycerol for clearing and mounting.

Results

Ablation of any mesoderm or ectoderm generating blastomere at the eight-cell stage can result in a viable hatchling

Fate mapping as well as detailed descriptions of early cell movements from the eight-cell stage in *P. hawaiensis* shows that cell lineages are essentially invariant and give rise to the germ layers in a stereotypical manner (Fig. 1; Gerberding et al., 2002; Price and Patel, 2008). If development were mosaic, then ablation of individual cells would result in an incomplete embryo lacking structures derived from the ablated lineage. On the other hand, if development of *Parhyale* is regulative, the remaining lineages will compensate for this loss and development of the embryo will be complete.

To test these possibilities, we first phototablated individual blastomeres and then allowed embryos to develop to hatching. We find that photoablation of any one of the six mesoderm or ectoderm generating blastomeres, at the eight-cell stage, can result in a fully formed and viable animal. In these animals, none of the ablated tissues are missing demonstrating that the remaining blastomeres must be able to compensate for this loss.

Compensation between mesoderm and ectoderm lineages is not observed following ablation at the eight-cell stage

To determine which lineages are able to compensate for the ablation of specific blastomeres, we combined ablation with lineage tracing experiments to uncover patterns of compensation during the development of mesoderm and ectoderm-ablated embryos. At the third cleavage, the ml and mr micromeres derive from an asymmetric division in which their sibling macromeres become ectodermal precursors (El and Er, respectively) (Gerberding et al., 2002). Therefore, we first sought to determine whether this relationship was retained such that ectoderm lineages might compensate for the loss of sibling mesoderm lineages. To do this, we injected mRNA encoding nuclear localized DsRed (DsRed-NLS) into one blastomere to act as a lineage tracer allowing us to track the origin of any compensating cells and ablated another blastomere as previously described.

We find that labeled El or Er lineages never give rise to mesodermal derivatives when the sister mesoderm micromere was ablated ($n=5/5$; data not shown). Therefore, the E macromere lineages do not compensate for ablated m micromere lineages. In the reciprocal experiment, when an E macromere is ablated and the sister m micromere labeled, we never observe the labeled mesodermal lineage giving rise to ectodermal cells ($n=28/28$; data not shown). These results show that compensation is not occurring between mesoderm and ectoderm sister blastomeres.

Ablation of a mesoderm blastomere – Mav, ml or mr – at the eight-cell stage is compensated for by the nonablated mesodermal lineages

We then tested whether it was the other mesodermal lineages that were able to compensate for the loss of a mesoderm blastomere. Normally, the Mav blastomere gives rise to the visceral mesoderm that surrounds the midgut anlagen as well as somatic head mesoderm anterior to mx2 (Browne et al., 2005; Figs. 2A, B–B″), while the ml and mr micromeres give rise to the mesoderm posterior to and including mx2 on the left and right sides, respectively, via a stereotyped lineage pattern that includes the asymmetric division of mesoteloblast cells into mesoblasts which then divide and further differentiate into segmental mesoderm (Gerberding et al. 2002; Price and Patel, 2008; Figs. 2G, H–H″).

First we tested whether Mav, the only macromere that gives rise to mesoderm, can compensate for loss of ml or mr lineages. In the ml or mr ablated embryos, we find that the DsRed-injected Mav lineage gave rise to labeled mesoteloblasts on the ablated side of the elongating germband, replacing the ablated lineage ($n=14/14$; Figs. 2C, D–D″). When both ml and mr micromeres are ablated at the eight-cell stage, the progeny of Mav is able to compensate for the segmental mesoderm on both left and right sides of the germband ($n=9/9$; Figs. 2E, F–F″). These results show that Mav is capable of producing mesoderm in segments posterior to and including mx2 in ablated animals. Interestingly, in these ablations, we never observe the progeny of ml compensating for mr or vice versa.

We next tested whether ml and mr were able to compensate for ablation of Mav. When we ablate Mav with concurrent labeling of ml or mr, we find that ml and mr are able to compensate for Mav loss ($n=14/14$; Figs. 2I, J–J″). This indicates that the ml and mr lineages can produce the full complement of visceral and somatic mesoderm anterior to mx2. Moreover, in these ablations, ml/mr progeny produce compensating mesoderm only on the left or right sides, respectively, of the visceral mesoderm, implying a spatial restriction in the pattern of compensation. This restriction is overcome when Mav and either ml or mr are ablated. In these cases, we observed that the remaining m micromere was able to compensate for the visceral mesoderm on both the left and right sides as well as the mesoderm in segments anterior to mx2 and the mesoteloblasts on the ablated side ($n=7/7$; Figs. 2K, L–L″). These results show that the mesoderm blastomeres – Mav, ml and mr – compose a mesoderm group (M) that is capable of intra-germ layer compensation.

Fig. 2. Mesoderm compensation following ablation at the eight-cell stage. All embryos are ventral views of germband stage embryos except for (A, C, E, G, I, K) which are vegetal views at the eight-cell stage. (A, C, E, G, I, K) Schematic at the eight-cell stage showing which cells have been ablated with FITC (black) or labeled with nuclear DsRed (red). Live dark-field image with fluorescent image overlay (B, D, F, H, J, L) or fluorescence only (B′, D′, F′, H′, J′, L′) to show orientation of cells in the context of the developing embryo. Embryos in this panel range in stage from S12 to S15, thus display a varying number of mesoblast rows in the different images. (B″, D″, F″, H″, J″, L″) Schematic of germband stage embryos indicating the observed lineage pattern (red) resulting after injection and/or ablation. (B, B′) The Mav lineage gives rise to visceral mesoderm observed as two bilateral spheres. (D, D′) When mr is ablated, labeled Mav cells compensate for loss of the mesoteloblasts (MTB) and mesoblasts (MB) on the right side (blue arrowhead). (F, F′) When ml and mr are both ablated, labeled Mav progeny compensate for MTB and MB (blue arrowheads) on both left and right sides. (H, H′) The ml lineage gives rise to the somatic mesoderm on the left side. (J, J′) In a Mav ablation, labeled ml cells give rise to the visceral mesoderm (blue arrow) on the left side. (L, L′) In a Mav and mr ablated embryo, the only remaining mesoderm lineage, ml (labeled), gives rise to the entire visceral mesoderm on both sides (blue arrows), as well as the somatic mesoderm on the right side (blue arrowhead). Scale bars: 100 μm.

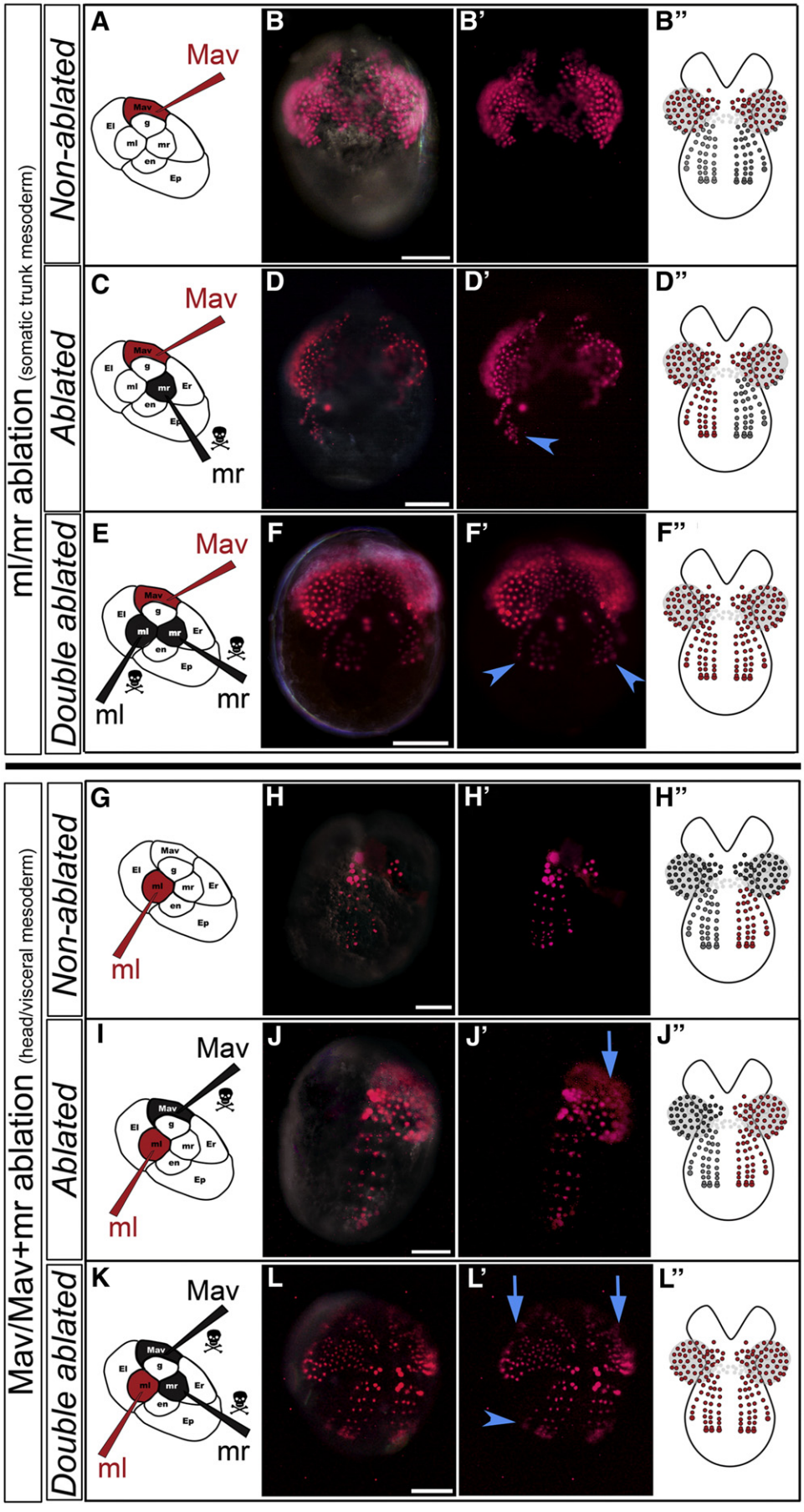
ml/mr ablation (somatic trunk mesoderm)
Non-ablated
Ablated
Double ablated
Mav/Mav+mr ablation (head/visceral mesoderm)
Non-ablated
Ablated
Double ablated
A
B
B'
B''
C
D
D'
D''
E
F
F'
F''
G
H
H'
H''
I
J
J'
J''
K
L
L'
L''
Mav
mr
ml
El
g
Er
en
Ep

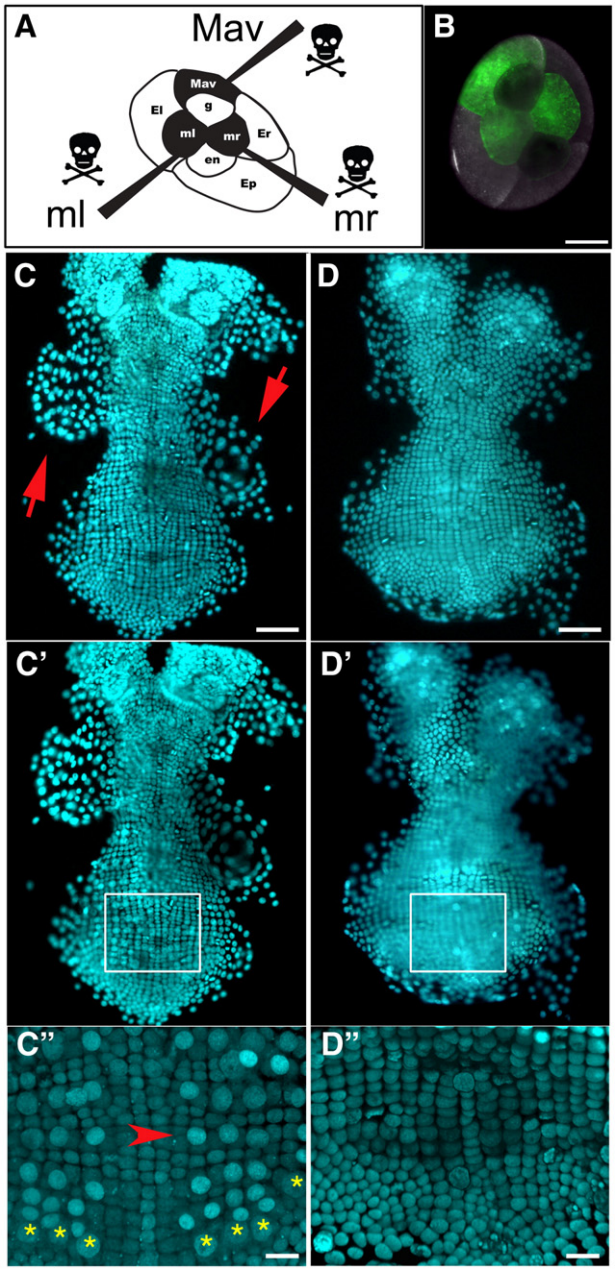

Fig. 3. Lack of compensation following ablation of the three mesoderm blastomeres at the eight-cell stage. (A) Schematic showing ablation of Mav, ml and mr. (B) Live image of eight-cell embryo injected with FITC dextran (green) in ml, mr and Mav before ablation. (C–D″) Ventral views of S15 DAPI-stained embryos. (C) Nonablated embryo at germband elongation focusing on the ectoderm. Red arrows indicate the visceral mesoderm, (C′) the underlying visceral and segmental mesoderm and (C″) confocal stack of the area in C′ (box) clearly showing the rows of mesoteloblasts (*) and mesoblasts (red arrowhead points to one of the rows of mesoblasts). (D) Triple mesoderm-ablated embryo focusing on the ectoderm, (D′) the underlying plane where mesoderm is usually found and (D″) confocal stack of area in D′ (box) showing the loss of mesoteloblasts and mesoblasts in ablated embryos. Loss of the visceral mesoderm is evident in D, D′. Scale bars: 100 μm, except in (C″, D″): 20 μm.

Ablation of the three mesoderm blastomeres – Mav, ml and mr – are not compensated for by any other lineages

To further support our hypothesis of a mesoderm group, we ablated all three mesoderm producing blastomeres (Mav, ml and mr) at the eight-cell stage. When all three mesoderm blastomeres were ablated at the eight-cell stage (Figs. 3A, B), there was a complete loss of mesoderm. Compared to nonablated embryos in which mesodermal derivatives such as the mesoteloblasts, mesoblasts and visceral mesoderm could easily be identified (Figs. 3C–C″) in triple-ablated embryos, these derivatives were absent from the germband ($n=8/8$; Figs. 3D–D″). These results suggest that none of the remaining blastomere derivatives can produce mesoderm and thus confirming that the ml, mr and Mav blastomeres are the only cells that will give rise to mesoderm from the eight-cell stage. Interestingly, ablation of these three blastomeres did not interfere with the embryos ability to gastrulate and form an elongating ectodermal germband suggesting there is little, if any, instruction from the mesoderm to the ectoderm during the initial phase of germband formation (stages 8–12). Later roles could not be assessed as these embryos died by stage 13 (70 h post fertilization [hpf]).

Ablation of an ectoderm blastomere – El, Er or Ep – at the eight-cell stage is compensated for by the nonablated ectodermal lineages

Given the presence of the mesoderm group, we next wanted to see if a similar relationship exists among the ectodermal lineages. Recall that the ectoderm in *Parhyale* is generated from three specific macromeres at the eight-cell stage: El, Er and Ep (Fig. 1). Each ectodermal macromere gives rise to a spatially restricted clone of cells in the left, right and posterior regions of the embryo, respectively (Gerberding et al., 2002; Fig. 1). To determine if the remaining ectodermal lineages compensate for the loss of an ectoderm blastomere, we photoablated one ectoderm blastomere and labeled a different ectoderm blastomere with the lineage tracer DsRed-NLS at the eight-cell stage. Our results show that the loss of any ectoderm blastomere is compensated for by the progeny of the remaining two ectoderm blastomeres in a predictable way. Normally, the El and Er blastomeres give rise to the left and right head ectoderm as well as portions of the left and right thoracic ectoderm, respectively (Figs. 4A, A′). The extent to which El or Er clones comprise the thoracic region varies between embryos with the remainder of the region being comprised of cells from the Ep lineage (Figs. 4B, B′; Gerberding et al., 2002). Labeling of El and ablation of Er or vice versa at the eight-cell stage resulted in labeled cells throughout the head region anterior to and including the anterior compartment of maxilla (mx1) of the developing germband, but not in the region posterior to the anterior compartment of mx1 of the ablated side ($n=7/7$; Figs. 4C, C′). As the region posterior to the anterior compartment of mx1 is normally formed in the El or Er ablated embryos, we expected that the cells compensating in this region might come from the lineage of the Ep blastomere which normally generates the posterior thoracic and abdominal ectoderm as well as the majority of the midline cells. Indeed, ablation of either the Er or El blastomere results in an extension of the labeled Ep lineage up to and including the posterior compartment of mx1, which is normally occupied by the ablated lineage ($n=8/8$; Figs. 4D, D′). Given this result, we then tested whether the reciprocal ablation would extend the lineages of El and Er posteriorly when Ep was ablated. We find that ablation of Ep and labeling of El or Er results in labeled progeny that occupy the entire left or right side of the germband, respectively, extending into the regions that are normally comprised of Ep lineage cells ($n=5/5$; Figs. 4E, E′). Strikingly, the compensating cells from El or Er do not cross the midline. Further, when a single ectoderm blastomere is ablated and the remaining two are labeled, we find the entire ectoderm of the resulting embryo is labeled confirming that the remaining two ectoderm blastomeres fully compensate for the loss of the third ($n=2/2$; Figs. 4F, F′). Embryos in which two ectoderm blastomeres are ablated do not survive to even an early germband stage; therefore, we cannot test whether the progeny of a single ectoderm blastomere is able to fully compensate for the loss of the other two ectoderm blastomeres, as is observed with the mesoderm.

In order to further investigate the patterns of the intra-germ layer compensation observed, we analyzed the localization of the lineage tracer in fixed specimens, rather than in live embryos, using an

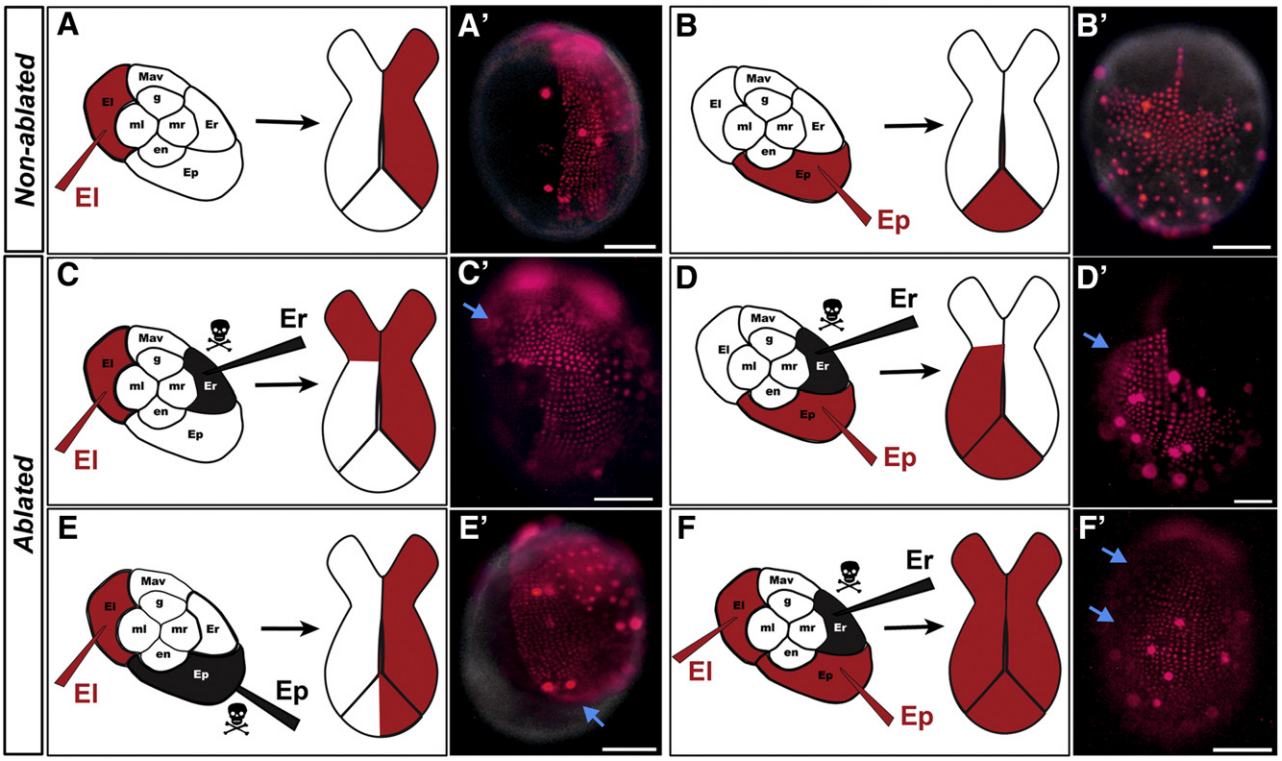

Fig. 4. Ectoderm compensation following ablation at the eight-cell stage. (A–F) Schematics of ablation (S4) and pattern of compensation (S15). Ablated blastomeres are in black; DsRed labeled lineages are in red. (A′–F′) Live fluorescent images of DsRed labeled and ablated embryos at germband elongation stages (S12–S15). Ventral views. Blue arrow indicates region of compensation. (A, A′) Labeling shows that the left ectoderm lineage maintains a boundary at the midline. The larger labeled nuclei are vitellophages underlying the germband that are also generated from the E blastomeres. (B, B′) Labeling shows the Ep lineage gives rise to the posterior ectoderm and midline. (C, C′) In an Er ablated and El labeled embryo, El compensates for the right ectoderm in the region anterior to and including the anterior compartment of mx1 (arrow). (D, D′) In Er ablated embryos, labeled Ep cells compensate for the ablated lineage on the right side of the germband, posterior to the anterior compartment of mx1 (arrow). (E, E′) In an Ep ablated and El labeled embryo, El compensates in the left posterior ectoderm (arrow). (F, F′) In Er ablated embryos where both El and Ep are labeled, the entire germband is labeled, with compensating cells presumably derived from El in the region anterior to and including the anterior compartment of mx1 (top arrow) and those from Ep in the region posterior to the anterior compartment of mx1 (bottom arrow), respectively. Scale bars: 100 μm.

antibody to DsRed at older stages of development (Fig. 5). By stage 19 (96 hpf), the germband is completely segmented and the appendages are becoming well defined and identifiable (Browne et al., 2005). Control embryos labeling the lineages of Er (Figs. 5A, A′), Ep (Figs. 5C, C′) and El (Figs. 5E, E′) show the typical lineage pattern of each of these blastomeres. Interestingly, following ablation, the pattern of Er and El lineage compensation appeared limited to the head region anterior to and including the anterior compartment of mx1 (Figs. 5B, B′), while the extent of Ep compensation was restricted to the region posterior to the anterior compartment of mx1 (Figs. 5D, D′), thereby supporting the parasegmental boundary of compensation seen in younger embryos (Figs. 4C, C′ and Figs. 4D, D′). In the case of compensation for posterior ectoderm normally made by Ep, a strict adherence to the left–right boundary was maintained, so that El compensated for the left posterior ectoderm (Figs. 5F, F′) and Er compensated for the right posterior ectoderm (data not shown). The cells that make up the midline were composed to varying extents of both the left and right ectoderm lineages in these ablated embryos. These results were intriguing because lineage studies of the ectoderm blastomeres at the 16-cell stage in *Parhyale* reveal a similar finding—that there is a parasegmental boundary between the anterior and posterior compartments of mx1 that segregates the ectoderm derived from El or Er into anterior and posterior regions (Figs. 5G–H′). In addition, our lineage studies show that the progeny from the daughter cells that result from division of Ep, Ep-l and Ep-r are segregated on the left and right sides of the germband, respectively, with the midline cells arising from either Ep-l or Ep-r or from both clones (Figs. 5I, I′). These anterior–posterior and right–left boundaries correspond to the patterns of compensation and boundaries we observe among the ectodermal lineages in ablated embryos.

These results show that the El, Er and Ep blastomeres constitute an ectoderm group (E) capable of intra-germ layer compensation. In addition, we also find stereotypical spatial restrictions among these ectoderm lineages. Although we find it unlikely, we cannot confirm that in the complete absence of the ectoderm other lineages may be able to compensate because embryos in which all three ectoderm blastomeres are ablated do not survive. Taken together, these results suggest that at the eight-cell stage a complete separation of ectoderm and mesoderm fate occurs and cell contribution to germ layers is already restricted.

Intra-germ layer compensation can occur as late as gastrulation

Having established that there are mesoderm and ectoderm groups that exist at the eight-cell stage, we wanted to know how late into development compensation could occur. An advantage of the photoablation technique is that it allows us to successfully ablate these cells at different developmental stages. By injecting blastomeres at the eight-cell stage with FITC and performing ablations at later time points in development, we were able to determine the degree to which the nonablated lineages were able to compensate at various stages of development. Using this approach, we first ablated blastomere progeny during gastrulation stage 8 (20–24 hpf) in order to determine if compensation could still occur following ablation at this stage.

At gastrulation, each ml and mr clone consists of about six cells. Following photoablation, these cells cease division and by 48 h post ablation, their debris is no longer visible in the embryo. In gastrulation stage ml or mr lineage-ablated embryos, we observe compensation of mesoteloblast development by the progeny of Mav, but not by the

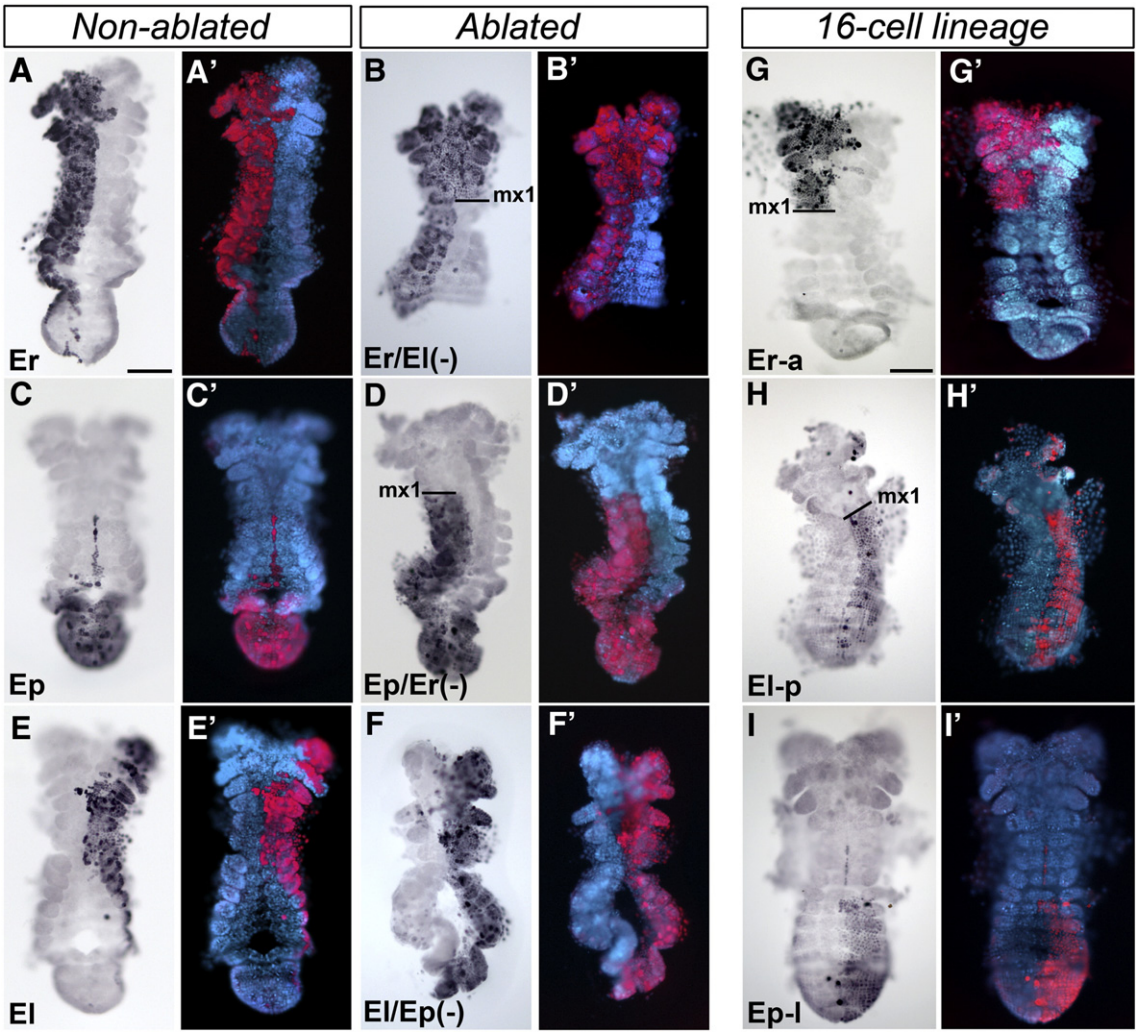

Fig. 5. Pattern of compensation in ectoderm-ablated embryos. Ventral views. Anterior is up. Pattern of compensation in ectoderm-ablated embryos: (A–I) Bright-field images of S19/20 anti-DsRed-stained embryos. (A′–I′) False color overlay of anti-DsRed staining on embryos counterstained with DAPI. (A, A′) In a control Er labeled embryo, labeled cells are primarily restricted to the right side of the germband. Notice some mixing in the head region. (B, B′) In an El ablated and Er labeled embryo, the Er lineage compensates for the loss of El in the region anterior to and including the anterior compartment of mx1 (black bar). The posterior most segments are missing due to dissection misfortune. (C, C′) In a control Ep labeled embryo, cells are restricted to the posterior ectoderm and midline cells. (D, D′) In an Er ablated and Ep labeled embryo, the posterior ectoderm compensates for the loss of El in the region posterior to the anterior compartment of mx1. (E, E′) In a control El labeled embryo, labeled cells are restricted to the left side of the germband. (F, F′) In an Ep ablated and El labeled embryo, the El lineage compensates for the loss of Ep in the posterior germband on the left side. Lineage pattern from the 16-cell stage ectodermal cells: (G, G′) In a control Er-anterior (Er-a) labeled embryo, labeled cells extend to and include the anterior compartment of mx1. (H, H′) In a control El-posterior (El-p) labeled embryo, labeled cells occupy the region posterior to the anterior compartment of mx1. (I, I′) In an Ep-left (Ep-l) labeled embryo, labeled cells are restricted to the left side of the midline. The lineages of the ectodermal blastomeres from the 16-cell stage reflect the boundaries observed between the anterior and posterior compartments of mx1 and at the level of the thoracic midline in ablated embryos. Scale bar: 100 μm.

remaining m micromere—identical to the situation seen in ablations at the eight-cell stage ($n=10/10$; see Figs. 2D–D″).

At gastrulation, the Mav lineage normally consists of approximately ten cells. Following ablation of the Mav lineage at gastrulation, the progeny of ml and mr are able to compensate for the ablated lineage—again identical to the situation seen for ablations at the eight-cell stage ($n=14/14$; see Figs. 2J–J″).

Within the E lineages, the same pattern of compensation is observed in gastrulation stage ablated embryos as was seen in the eight-cell-stage ablated embryos (Supplementary Fig. 1). Each E clone (El, Er or Ep) consists of approximately 27–31 cells at gastrulation. These ectoderm clones are organizing into a germ disc and are already spatially organized into left, right and posterior regions (Browne et al., 2005). Ablation of ectoderm clones at gastrulation results in embryos that are severely developmentally delayed, particularly on the ablated side, and as a consequence develop asymmetrically. Briefly, ablation of either Er or El progeny are compensated for by the progeny of El or Er, respectively, in the region anterior to and including the anterior compartment of mx1, while the progeny of Ep compensates for the loss of cells in the region posterior to the anterior compartment of mx1 ($n=8/8$); ablated Ep progeny are compensated for by the El and Er lineages ($n=4/4$) in the posterior thoracic and abdominal region. Moreover, in the case of the gastrulation stage ectoderm ablations, the pattern of compensation continues to be spatially restricted to observe the left–right boundary in the thoracic region as well as a parasegmental boundary between the anterior and posterior compartment of mx1, as observed in ablations performed at the eight-cell stage. These results show that compensation among germ layer groups occurs as late as gastrulation in a predictable manner.

Intra-germ layer compensation does not occur at germband stages

We next wanted to determine if there was a time in development when compensation in the mesoderm or ectoderm lineages did not occur. Using the same technique for ablations at gastrulation, we

ablated blastomere progeny at the beginning of germband elongation at stage 10/11 (56–60 hpf).

ml or mr lineage ablations performed just after formation of the mesoteloblasts at germband elongation stage 10/11 (56–60 hpf; Figs. 6A, B) resulted in no compensation for the ablated lineage ($n=23/23$). The *Parhyale* ortholog of *myocyte enhancing factor 2* (*Ph-mef2*), a marker of differentiated mesoderm (Price and Patel, 2008), was completely absent on the ablated side (Figs. 6C, C′) compared to the nonablated side and control embryo (Figs. 6D, D′), demonstrating the loss of body musculature. Although these animals were able to develop to late germband stage 24 (155 hpf), they never hatched.

When Mav progeny were ablated at stage 10/11 (Figs. 6E, F), they were not compensated for by the progeny of ml and mr, resulting in a loss of the visceral mesoderm ($n=6/6$). These embryos often continued to develop; some developing as late as stage 26 (180 hpf). However, the midgut and digestive cecae clearly did not form in ablated embryos (Figs. 6G, H) compared to nonablated embryos (Figs. 6I, J). Based on these observations, compensation of ablated mesodermal lineages does not occur following ablation at germband stages.

Ablation of the ectoderm lineages derived from El or Er ($n=17/17$; Figs. 7A, B) or Ep ($n=9/9$; Figs. 7D, E) at the germband elongation stage 10/11 results in a permanent loss of that tissue, suggesting that at this stage, the other ectoderm cells are not able to compensate. Typically these embryos are severely affected and die during germband elongation. Occasionally, some embryos reach stages 21–23 (120–144 hpf), but these embryos lack the segments and appendages from the ablated region (Figs. 7C, F) compared to the nonablated side or nonablated embryos (Fig. 7G). The severity of

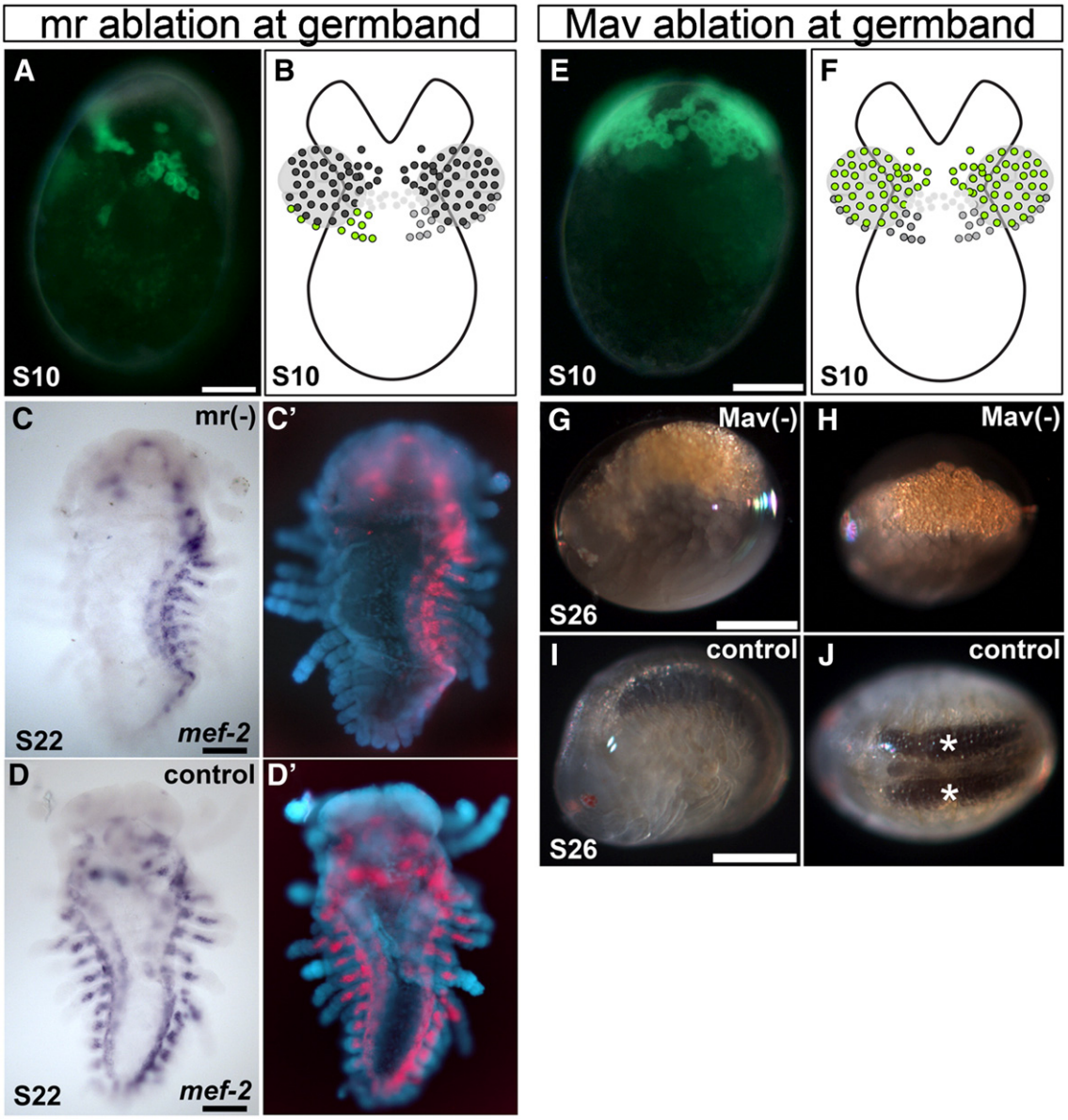

Fig. 6. Ablation of mesoteloblasts and visceral mesoderm at germband stage. (A, E) Live image and (B, F) schematic of S10 embryo at time of ablation of mr or Mav lineage (green cells). (C, D) Bright-field image of *Ph-mef-2 in situ* in mr ablated (C) and nonablated (D) embryos at S22. (C′, D′) Corresponding false color overlay with DAPI. (A–F) Ventral views. (G–J) Bright-field images showing development of the midgut or digestive cecae in Mav lineage-ablated (G, H) and control (I, J) embryos at S26. Anterior is to the left. (G, I) Lateral views. (H, J) Dorsal views. (A, B) The four mesoteloblasts which gives rise to the segmental mesoderm have just formed at S10. (C) Ablation of mr progeny at S10 results in the loss of segmental mesoderm as shown by the loss of expression of a muscle determination marker, *Ph-mef2* on the ablated side. (D) A nonablated embryo stained for *Ph-mef2*. (E, F) At S10, Mav progeny are present at the level of the forming midgut anlage as two circular masses of cells. (G, H) Ablation of Mav at germband stages results in embryos lacking a midgut or digestive cecae. (I, J) Nonablated embryo with the midgut and bilateral cecae formed (asterisks). Scale bars: 100 μm.

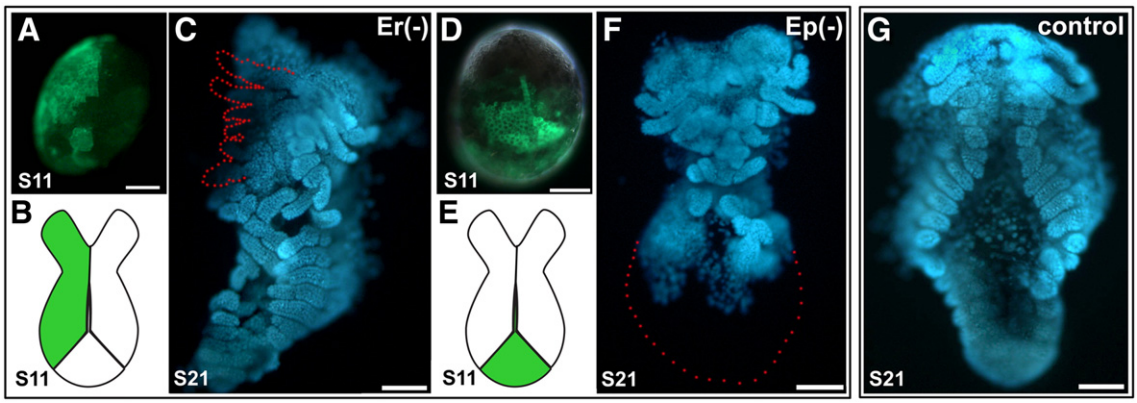

Fig. 7. Ablation of the ectoderm lineages at germband stage. Ventral views. (A, D) Fluorescent live images of S11 germband staged embryos at the time of ablation (green = FITC). (B, E) Schematic of panels A and D, respectively. DAPI images of (C, F) S21 ablated and (G) nonablated embryos. (C) In an Er-germband ablated embryo there is a loss of anterior right segments and limbs. The severity of loss varies between embryos based on the size of the ectodermal clone at time of ablation. In this case, this embryo has lost six anterior segments on the right side (lost area represented by red outline). (F) Ep-germband ablated embryo. Ablation of the posterior ectoderm results in a complete loss of posterior segments on both right and left sides (lost area represented by the red outline). (G) Control embryo. Scale bars: 100 μm.

the defects depends on the size of the clone at the time of ablation, which varies greatly among embryos.

These results show that by the beginning of germband elongation, compensation for the loss of ectoderm or mesoderm lineages no longer occurs suggesting that, between the beginning of gastrulation and the beginning of germband elongation in *Parhyale,* portions of the germ layers have become committed.

Discussion

Mesoderm and ectoderm groups in Parhyale at the eight-cell stage

Due to its invariant cell lineage and ease to maintain and manipulate in the laboratory, *P. hawaiensis* presents itself as an attractive organism in which to explore the molecular mechanisms behind early specification of germ layers and axes. Here, our results demonstrate that, although early lineages are restricted, the early development of the *Parhyale* embryo is also highly regulative. We show that ablation of a mesoderm or ectoderm generating blastomere at the eight-cell stage or its progeny at gastrulation can be compensated for by cells of other lineages in a stereotypical pattern.

In *Parhyale*, regulation of ablated lineages does not occur by inter-germ layer compensation, but rather is restricted to specific germ layer groups established at the third division. Our labeling and ablation experiments show intra-germ layer compensation, such that mesodermal cells can only compensate for loss of other mesodermal cells while ectodermal cells can only compensate for loss of other ectodermal cells. This demonstrates that at the eight-cell stage in *Parhyale*, at least two germ layer groups are established: the mesoderm group (Mav, ml and mr or M) and the ectoderm group (El, Er and Ep or E). Our results suggest that these groups are not present until the eight-cell stage and, indeed, in cell separation studies it has been reported that each blastomere isolated at the two-cell stage will continue to divide asymmetrically and can develop at least to gastrulation and form multiple cell layers in *Parhyale* (Extavour, 2005). Thus, it is not until the third cleavage that the germ layer potential of blastomeres becomes set. Equivalence groups are groups of cells that will eventually contribute to different derivatives, but at an earlier point in development, all have the same developmental potential. Only after subsequent inductive events do they reach their final state of differentiation (Kimble, 1981). It is possible that the germ layer groups seen in *Parhyale* may constitute equivalence groups as seen in *C. elegans* and ctenophores (Kimble, 1981; Henry and Martindale, 2004). Further studies uncovering the molecular mechanisms allowing for proper compensation among these different cell lineages will shed more light on this distinction.

The observed intra-germ layer compensation of cells suggests that the embryo possesses mechanisms to assess the status of germ layers and can respond to replace missing tissue or cell types. As may be expected, the regulative ability of both groups diminishes as development proceeds. This decrease in regulative ability culminates in the interval between gastrulation and germband elongation where the embryo loses the ability to replace ablated cells. Clearly, much of the commitment of cells to their final fate has occurred by this time. The ability of embryos to regulate until gastrulation suggests that there must be cell–cell communication within the M and E groups that can lead to changes in cell behavior. Also, the developmental lag in compensating regions suggests that developmental patterning of these regions is slowed, perhaps waiting for completion of a developmental checkpoint. In compensated embryos, one can assume that cell proliferation will need to be locally increased to replace missing cells, however the selection of cells that are to proliferate may be a critical step. The path along which the two germ layers normally develop may provide insight into different mechanisms that could be more important for compensation. For example, within the mesoderm group, the compensated cells are divided into two distinct cell fates: the visceral mesoderm or the segmental mesoderm. The critical "checkpoint" for mesoderm compensation may be regulated primarily by cell fate specific cues. On the other hand, the ectoderm behaves as an epithelial sheet. Perhaps, the compensation of cells from an ablated ectoderm blastomere is primarily driven by physical cues that drive local proliferation to fill in the gap left by the ablated lineage. It will be of great interest to understand the molecular signals behind these checkpoints and how they fit into the germband elongation program generally.

Presence and significance of the boundary between the anterior and posterior compartments of maxillary 1 in the ectoderm and somatic mesoderm

The ectoderm of the *Parhyale* germband can be subdivided into two main regions that have different properties: the nonordered cells of the head anterior to and including the anterior compartment of the first maxillary segment (mx1) and the highly ordered cells posterior to the anterior compartment of mx1 that are derived from rows of cells called parasegment precursor cell rows (PSPR) which undergo stereotypical divisions (Browne et al., 2005). These two distinct regions can be observed starting very early in development, before molecular markers of segmentation, such as Engrailed, are expressed

(Browne et al., 2005). Indeed, lineage studies performed a the 16-cell stage both here and in the amphipod *O. cavimana*, show that the daughter cells of the macromeres El and Er will give rise to an anterior and posterior region with the boundary of these clones dividing the mx1 segment (i.e., a parasegment boundary), suggesting that this boundary may be set up very early in development (Wolff and Scholtz, 2002). Excitingly, our ablation experiments show that cells compensating for the loss of either El or Er also do not appear to cross this particular parasegmental boundary. While this result could be explained by the rate of cell division and embryonic architecture limiting the regions in which compensation may occur, the 16-cell lineage studies and the striking difference between the two groups of cells suggests that the regulative capacity of ectodermal blastomeres at the 16-cell stage may not be equal (Browne et al., 2005; Wolff and Scholtz, 2002). Either an inductive event or a differentially distributed cytoplasmic determinant might define anteroposterior potential of these blastomeres at this stage. Indeed, more evidence for these possibilities is provided by ablation experiments at gastrulation stages where the same parasegmental boundary of compensation from the eight-cell stage is retained. However, future ablation experiments coupled with a molecular characterization of compensation will elucidate whether these boundaries are functional or coincident. It will be of great interest to see what genes are expressed from the eight-cell stage through the establishment of this boundary and if their knockdown or overexpression cause changes in ectoderm germband growth or identity.

Similar to the ectoderm, the somatic mesoderm can be subdivided into two main regions that have different properties: nonordered cells anterior to mx2 that are not derived from mesoteloblast divisions and the highly ordered cells posterior to and including mx2 that are derived from the divisions of the mesoteloblasts (Browne et al., 2005; Price and Patel, 2008). Interestingly, the mesodermal cells derived from the mesoteloblasts in mx2 are underneath the anterior compartment of mx2, which is in the same parasegment as the posterior compartment of mx1 (i.e.: the boundary between the two types of ectoderm and mesoderm is the same for both tissues). It will be of great interest to see if the same mechanism sets up this boundary in both the ectoderm and the mesoderm.

Germ layer specification by induction or localization of determinants

The establishment of these germ layer groups so early in development, even before the establishment of multiple layers of cells is striking and indicates that the earliest cleavages may be highly polarized. It is unclear what mechanisms are involved in these polarized cell divisions, for example, whether maternal determinants are placed asymmetrically in the egg as in *Drosophila* (Anderson and Nusslein-Volhard, 1984; St Johnston and Nusslein-Volhard, 1992) or whether some impetus from the sperm entry point is responsible for establishing this polarity as in nematodes and ascidians (Bates and Jeffery, 1988; Goldstein and Hird, 1996; Jeffery, 1982).

There is evidence that supports a combination of mechanisms in *Parhyale*. First, there are visible asymmetries at the one-cell stage that are associated with later polarity. Polar bodies, which in other organisms are formed just following activation of the egg by sperm, are clearly associated with the initial cleavage plane and the subsequent development of the ectodermal blastomeres or “animal” hemisphere (Browne et al., 2005). Second, maternally loaded factors may also be important in *Parhyale*. On the “vegetal” side of the one-cell embryo, opposite to the polar bodies, is a small island of cytoplasm that marks the pole where micromeres will develop. Indeed, at the eight-cell stage, the cytoplasm of the g micromere (which gives rise to germline) of *Parhyale* clearly looks different from the other cells (Gerberding et al., 2002). Furthermore, blastomere isolations showed that the localization of a germline marker is restricted to the lineage leading to the g blastomere (Extavour, 2005). It is therefore likely that early cell asymmetries and localized maternal factors play a role in specifying the mesoderm and ectoderm lineages.

Our experiments in *Parhyale* show that, although the restrictions of early cell lineages would suggest mosaicism, the intra-germ layer compensation observed demonstrates that regulation also occurs. This supports the view that during metazoan development a combination of early determinants and induction are more commonly used and that more often, sequential periods of cell autonomy followed by cell–cell interactions in a spatial and temporal context are important for specification. In order to further our understanding of the process of cell fate specification and germ layer compensation in *Parhyale*, the molecular events leading to the establishment of the germ layer groups and the subsequent signaling events occurring within germ layers need to be uncovered.

Acknowledgments

We would like to thank all the members of the Patel lab for helpful discussions. We especially give thanks to Meredith Protas, Paul Liu, Cristina Grande, Henrique Marques-Souza, Crystal Chaw and E. Jay Rehm as well as Dede Lyons and David Buckley for their valuable feedback on this manuscript. NHP is an Investigator of the Howard Hughes Medical Institute.

Appendix A. Supplementary data

Supplementary data associated with this article can be found, in the online version, at doi:10.1016/j.ydbio.2009.12.006.

References

Anderson, K.V., Nusslein-Volhard, C., 1984. Information for the dorsal–ventral pattern of the *Drosophila* embryo is stored as maternal mRNA. Nature 311, 223–227.

Anderson, K.V., Jurgens, G., Nüsslein-Volhard, C., 1985. Establishment of dorsal–ventral polarity in the *Drosophila* embryo: genetic studies on the role of the Toll gene product. Cell 42, 779–789.

Bates, W.R., Jeffery, W.R., 1988. Polarization of ooplasmic segregation and dorsal–ventral axis determination in ascidian embryos. Dev. Biol. 130, 98–107.

Browne, W.E., Price, A.L., Gerberding, M., Patel, N.H., 2005. Stages of embryonic development in the amphipod crustacean, *Parhyale hawaiensis*. Genesis 42, 124–149.

Extavour, C.G., 2005. The fate of isolated blastomeres with respect to germ cell formation in the amphipod crustacean *Parhyale hawaiensis*. Dev. Biol. 277, 387–402.

Gerberding, M., Browne, W.E., Patel, N.H., 2002. Cell lineage analysis of the amphipod crustacean *Parhyale hawaiensis* reveals an early restriction of cell fates. Development 129, 5789–5801.

Goldstein, B., Hird, S.N., 1996. Specification of the anteroposterior axis in *Caenorhabditis elegans*. Development 122, 1467–1474.

Henry, J.Q., Martindale, M.Q., 2004. Inductive interactions and embryonic equivalence groups in a basal metazoan, the ctenophore *Mnemiopsis leidyi*. Evol. Dev. 6, 17–24.

Hertzler, P.L., Clark Jr., W.H., 1992. Cleavage and gastrulation in the shrimp *Sicyonia ingentis*: invagination is accompanied by oriented cell division. Development 116, 127–140.

Hertzler, P.L., Wang, S.W., Clark Jr., W.H., 1994. Mesendoderm cell and archenteron formation in isolated blastomeres from the shrimp *Sicyonia ingentis*. Dev. Biol. 164, 333–344.

Jeffery, W.R., 1982. Calcium ionophore polarizes ooplasmic segregation in ascidian eggs. Science 216, 545–547.

Kimble, J., 1981. Alterations in cell lineage following laser ablation of cells in the somatic gonad of *Caenorhabditis elegans*. Dev. Biol. 87, 286–300.

Lawrence, P.A., Levine, M., 2006. Mosaic and regulative development: two faces of one coin. Curr Biol. 16, R236–239.

Levin, M., Thorlin, T., Robinson, K.R., Nogi, T., Mercola, M., 2002. Asymmetries in H+/K+-ATPase and cell membrane potentials comprise a very early step in left–right patterning. Cell 111, 77–89.

Patel, N.H., 1994. Imaging neuronal subsets and other cell types in whole-mount *Drosophila* embryos and larvae using antibody probes. Methods Cell Biol. 44, 445–487.

Price, A.L., Patel, N.H., 2008. Investigating divergent mechanisms of mesoderm development in arthropods: the expression of *Ph-twist* and *Ph-mef2* in *Parhyale hawaiensis*. J. Exp. Zool., B Mol. Dev. Evol. 310, 24–40.

Rehm, E.J., Hannibal, R.L., Chaw, R.C., Vargas-Vila, M.A., Patel, N.H., 2009. The crustacean

Parhyale hawaiensis: a new model for arthropod development. In: Crotty, D.A., Gann, A. (Eds.), Emerging Model Organisms: A Laboratory Manual. Cold Spring Harbor Laboratory Press, New York, pp. 373–404.
Rushlow, C.A., Han, K., Manley, J.L., Levine, M., 1989. The graded distribution of the dorsal morphogen is initiated by selective nuclear transport in *Drosophila*. Cell 59, 1165–1177.
Schnabel, R., 1997. Why does a nematode have an invariant cell lineage? Semin. Cell Dev. Biol. 8, 341–349.
Shankland, M., 1984. Positional determination of supernumerary blast cell death in the leech embryo. Nature 307, 541–543.
Speksnijder, J.E., Jaffe, L.F., Sardet, C., 1989. Polarity of sperm entry in the ascidian egg. Dev. Biol. 133, 180–184.
Spemann, H., Mangold, H., 1924. Uber Induktion von Embryonalanlagen durch Implantation artfremder Organisatoren. Arch. Mikrosk. Anat. Entwickl.mech. 100, 599–638.
St Johnston, D., Nusslein-Volhard, C., 1992. The origin of pattern and polarity in the *Drosophila* embryo. Cell 68, 201–219.
Sulston, J.E., Schierenberg, E., White, J.G., Thomson, J.N., 1983. The embryonic cell lineage of the nematode *Caenorhabditis elegans*. Dev. Biol. 100, 64–119.
Wolff, C., Scholtz, G., 2002. Cell lineage, axis formation, and the origin of germ layers in the amphipod crustacean *Orchestia cavimana*. Dev. Biol. 250, 44–58.
Zhang, J., Houston, D.W., King, M.L., Payne, C., Wylie, C., Heasman, J., 1998. The role of maternal VegT in establishing the primary germ layers in *Xenopus* embryos. Cell 94, 515–524.